JOURNAL OF MATERIALS SCIENCE 32 (1997) 1889–1894

Formation of $CuInSe_2$ by the selenization of sputtered Cu/In layers

D. BHATTACHARYYA, I. FORBES, F. O. ADURODIJA, M. J. CARTER
Newcastle Photovoltaics Applications Centre, Department of EEEP, University of Northumbria at Newcastle, Newcastle upon Tyne, NE1 8ST, UK

Single layers of Cu and In were deposited onto Mo coated glass substrates by radio frequency sputtering. The $Cu_{11}In_9$ phase has been found to be the majority phase in these precursors. The selenization of the sputtered layers has been achieved by depositing a 1 μm Se layer onto the precursor by thermal evaporation followed by an annealing in vacuum. Samples were annealed at different temperatures varying between 100–600 °C at intervals of 50 °C. The chalcopyrite structured ternary phase of $CuInSe_2$ with a significant amount of preferential orientation in the (112) direction was obtained in samples annealed at 400 °C or above. Morphological, compositional and structural analyses of the samples annealed at different temperatures were performed using a variety of complementary techniques. The results were analysed to explain the growth of $CuInSe_2$ on the selenization of sputtered Cu–In precursors. The occurrence of various binary phases of Cu–In, Cu–Se and In–Se in different annealing temperature ranges has also been investigated. The phenomenon of volume expansion in $CuInSe_2$ on selenization has been found to manifest itself as a shift in the characteristic (110) X-ray diffraction peak of Mo.

1. Introduction

$CuInSe_2$ and related chalcopyrite materials have been shown to be potentially good absorbers for efficient solar cell device fabrication. $CuInSe_2$ and $Cu(In, Ga)Se_2$ films deposited using various growth techniques have been incorporated into polycrystalline thin film solar cell devices [1–6] that have displayed efficiencies $> 10\%$ with a maximum reported value of 16.4% [2]. Most of the $CuInSe_2$ films used in these devices have been fabricated by the three source co-evaporation technique [4]. Despite the demonstration of feasibility of producing cells using this technique and the excellent efficiency results obtained in laboratory scale devices, there is still doubt regarding its acceptance as a large scale production technique due to the inherent cost and area uniformity problems. Other techniques that have been applied to grow device quality $CuInSe_2$ films include laser synthesis [7], screen printing [8], the stacked elemental layer (SEL) method [9] and sputtering [10–13].

Sputtering has several advantages over the other deposition processes including: (i) the composition of the sputtered material is the same as that of the substrate, (ii) the deposition conditions are very stable and easily controllable by the plasma current, (iii) the loss of materials is minimal and (iv) the heat load on the chamber wall is very small, thereby reducing outgassing and subsequent incorporation by the reactive particles. Thus compared to the thermal co-evaporation process sputtering offers a relatively straightforward large-area scale up method for thin film deposition. The radio frequency (rf) sputtering of compound $CuInSe_2$ targets [10], the reactive direct current (dc) magnetron sputtering of Cu–In elemental targets in the presence of H_2Se [11] and the three source magnetron sputtering of elemental Cu, In and Se [12, 13] have been utilized to grow $CuInSe_2$ films that can be incorporated into the fabrication of high efficiency solar cells [14].

The direct sputtering of the compound involves the preparation of a high quality stoichiometric $CuInSe_2$ target, while the sputtering of the three different elemental targets is limited by: (i) due to the low thermal conductivity of Se, hot spots can develop on the Se target which give rise to non-uniform sputtering and (ii) the formation of $Cu_{2-x}Se$ and In_2Se_3 on the surface of the metal targets reduces the sputtering yield of Cu and In by 50 and 20% respectively and (iii) the selenization of the sputtered layers using H_2Se is not desirable due to safety problems.

In this paper, we report on the deposition of device quality $CuInSe_2$ thin films by a hybrid process in which the selenization of the Cu–In precursor prepared by sputtering was achieved by the deposition of a layer of Se on to the precursor by thermal evaporation and a subsequent vacuum annealing.

2. Experimental procedure

The precursor alloy was deposited onto a Mo coated glass substrate using an rf magnetron sputtering system. The sputtering system contains a load lock

0022–2461

system and a rotatable substrate holder. The three target electrodes were planar 15 cm (6″) discs. The Cu and In targets were of high purity being 99.998 and 99.999% respectively and the deposition was performed using high purity argon. The precursor alloy was produced by the sequential deposition of a single Cu layer and a single In layer on to the Mo-coated glass substrate, and the overall film thickness was about 1 μm. A *circa* 1 μm thick Se layer was then thermally evaporated onto the precursor substrate at ambient temperature. This amount of Se is sufficient to completely react with the Cu–In metallic multilayer precursor to form $CuInSe_2$. The whole structure was then placed into a partially closed graphite box and was annealed in a glass quartz tube furnace under a vacuum of 1.333 Pa. Samples were annealed at different temperatures varying between 100–600 °C at intervals of 50 °C. All the samples were characterized by scanning electron microscopy (SEM), energy dispersive X-ray analysis (EDX) and X-ray diffraction (XRD).

3. Results and discussion

3.1. Morphological analysis

Fig. 1(a–c) consists of the surface SEM micrographs and Fig. 2(a–c) consists of the cross-sectional SEM micrographs of the samples annealed at different temperatures. For films annealed at lower temperatures the unreacted Se layer on top of the Cu–In layer can be clearly observed. With an increase in the annealing temperature the Se layer reacts with the Cu–In precursor to yield $CuInSe_2$. For samples annealed at 500 °C, as can be seen in Fig. 1(c), 1 μm size of triangular faced crystals are obtained that show a preferential growth in the (1 1 2) direction. This preferential growth direction was confirmed by the XRD analysis. It can also be observed from the cross-sectional micrographs, Fig. 2(a–c), that the thickness of the film decreases as the annealing temperature increases from 150 °C which shows that there is a significant loss of Se during the annealing at higher temperatures.

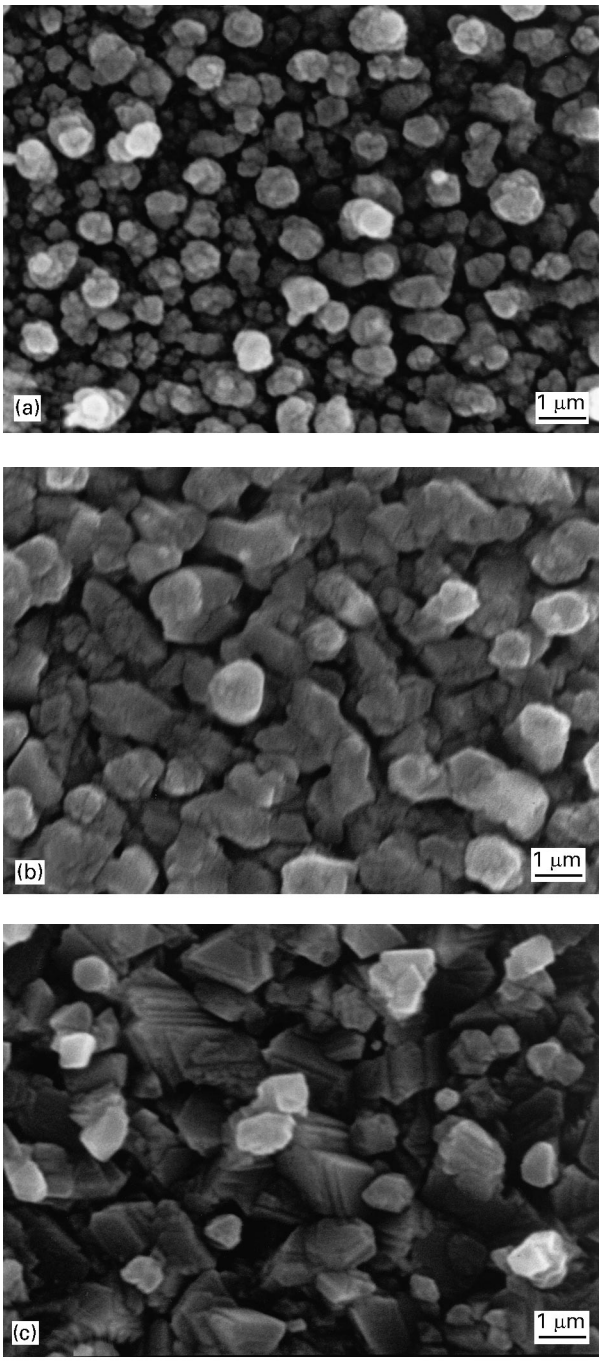

Figure 1 SEM micrographs of the films annealed at temperatures of: (a) 150 °C, (b) 300 °C and (c) 500 °C.

3.2. Compositional analysis

The assumption that there is a significant Se loss from the precursor during high temperature annealing is confirmed by the EDX compositional analysis. Fig. 3 shows the phase representation of the ternary compositional triangle for $CuInSe_2$ in terms of the binary compositions and the composition of the samples annealed at different temperatures. It is found that significant Se incorporation occurred in samples annealed at 100 °C, however with an increase in the annealing temperature a considerable amount of Se is lost from the samples and the composition approaches the stoichiometric value of $CuInSe_2$ for samples annealed at 400 °C or above. However, there is a further deviation from the correct stoichiometry when the annealing temperature exceeds 550 °C, with the production of secondary impurity phases that were observed in the XRD patterns.

3.3. XRD analysis

Fig. 4 shows the XRD pattern of a precursor layer which contains a significant amount of $Cu_{11}In_9$. The peaks that correspond to this phase are also observed in films after the growth of the Se layer although their heights decrease with an increase in the annealing temperature. Fig. 5(a) shows the variation of the normalized $Cu_{11}In_9$ peak with annealing temperature in the samples containing the Se layer. It has been previously reported by other groups working on the sputtered precursor/selenization process that a stable $Cu_{11}In_9$ majority phase needs to be present in the precursor layer if high quality $CuInSe_2$ films are to be produced [15]. $Cu_{11}In_9$ has been identified as being the most stable state in thin films of Cu/In alloys at higher temperatures, and in general any other unstable

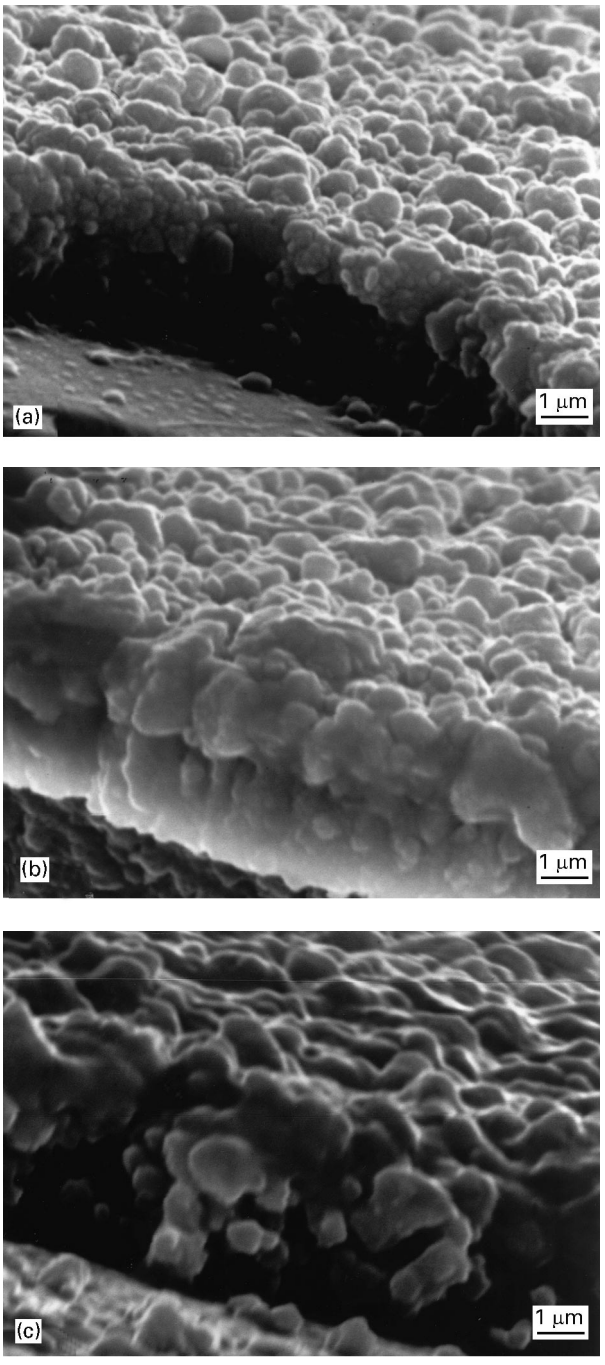

Figure 2 Cross-sectional SEM micrographs of films annealed at temperatures of: (a) 150 °C, (b) 300 °C and (c) 500 °C.

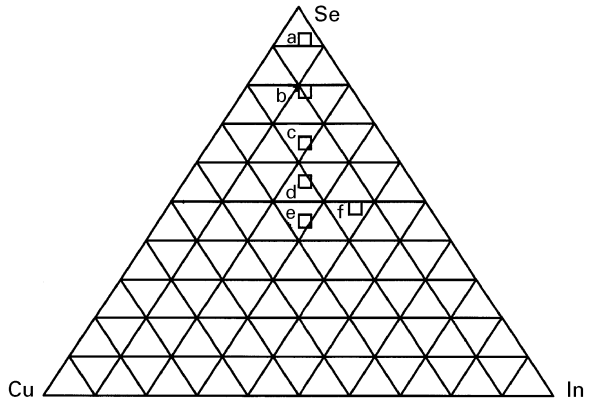

Figure 3 Compositions of the $CuInSe_2$ films annealed at temperatures of (a) 100 °C, (b) 200 °C, (c) 300 °C, (d) 400 °C, (e) 500 °C and (f) 600 °C represented in the ternary composition triangle.

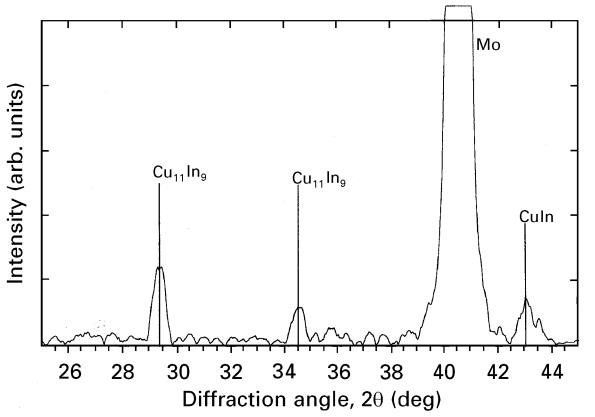

Figure 4 XRD pattern of the Cu–In precursor.

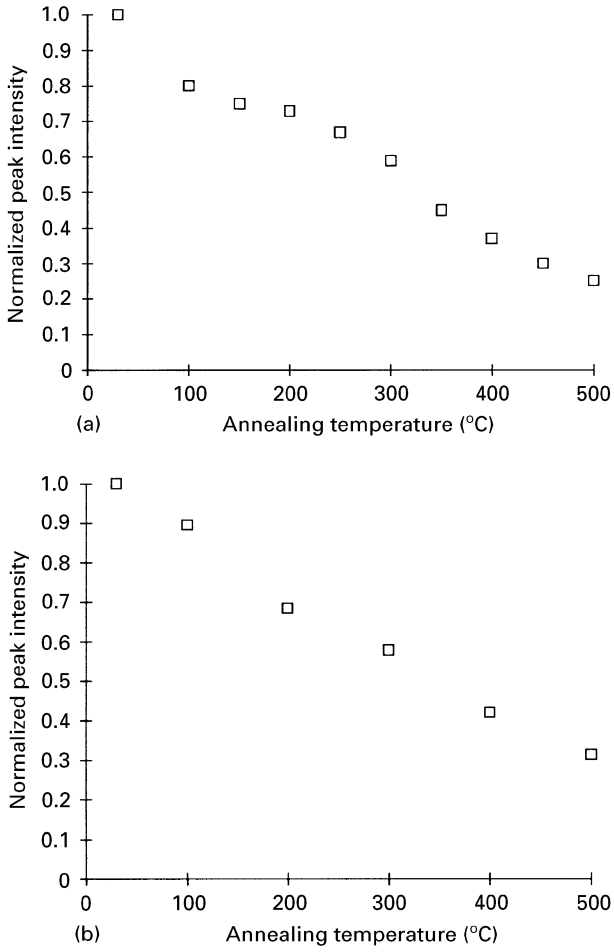

Figure 5 (a) Variation of the normalized intensity of the $Cu_{11}In_9$ peak with annealing temperature and (b) variation of the normalized intensity of the CuIn peak with annealing temperature and (a) 150 °C, (b) 250 °C.

Cu/In phases observed in the films tend to be transformed into $Cu_{11}In_9$. However, in the case of our samples, other binary phases of Cu and In, e.g., CuIn are also observed in the precursor layer (Fig. 4) and in the annealed samples. Fig. 5(b) shows the variation of the normalized peak of the CuIn phase which shows that the peak height decreases with an increase in the annealing temperature. The height of this peak decreases as the peaks associated with the $Cu_{16}In_9$ and Cu_9In_4 phases increase in the samples annealed in

the temperature range of 250–400 °C. These peaks that almost coincide with the (204/220) chalcopyrite peak of $CuInSe_2$, are found to be predominant at temperatures $\geqslant 250$ °C. However, the peak heights are reduced for samples annealed at temperatures above 400 °C due to the reaction of the Cu/In layers with the Se. Such a transformation of the CuIn phase to other phases at elevated substrate temperatures has been previously reported by other workers [15, 16]. It should however be noted that the Cu_4In and Cu_7In_4 phases reported by other workers for electrodeposited Cu–In layers have not been observed in our samples [17]. In addition no significant peaks of elemental In or Cu are observed which suggests that in our samples almost all of the Cu and In are in the form of $Cu_{11}In_9$ and other solid phases.

The development of the $CuInSe_2$ phase in the Cu–In–Se stack as a function of annealing was studied by observing the peaks associated with the different binary phases of Cu–Se and In–Se in the XRD patterns obtained for the samples. Significant peaks were observed that could be assigned to $CuSe_2$, In_2Se_3 and Cu_2Se. The $CuSe_2$ peak, which almost coincides with that of the $Cu_{11}In_9$ phase from the precursor, as can be seen from Fig. 6(a), is found to significantly increase in height at about 200 °C and then gradually decrease with annealing temperature. The α-In_2Se_3 peak is observed to appear in samples annealed above 200 °C and then decrease slightly with temperature [Fig. 6(b)]. An intense peak for α-In_2Se_3 at about ($2\theta = 27°$) is only observed in samples annealed at 300 °C. The appearance of In_2Se_3 at a substrate temperature of about 250 °C for $CuInSe_2$ films grown by magnetron sputtering of the three constituent elements has been reported by Nakada *et al.* [13]. It can be seen from Fig. 6(c), that β-In_2Se_3 is also present in significant quantities along with α-In_2Se_3 in samples annealed above 250 °C. Fig. 6(d) shows that the Cu_2Se peak, which almost coincides with the (1 1 2) peak of $CuInSe_2$, becomes significant for samples annealed at about 350 °C. It decreases at higher temperatures possibly due to the reaction of Cu_2Se with In_2Se_3, to form the ternary compound $CuInSe_2$. The characteristic peaks of the chalcopyrite form of $CuInSe_2$ are observed in the diffraction pattern of films annealed at temperatures of about 550 °C as is shown in Fig. 7. The peaks correspond to the (1 0 1), (1 1 2), (1 0 3), (2 1 1), (2 0 4/2 2 0) and (1 1 6/3 1 2) planes and the strength of the reflection from the (1 1 2) plane suggests that the crystals are strongly oriented in this plane. However, in films annealed at temperatures above 550 °C, some unstable phases of the type $(CuSe_2)_x$–$(In_2Se_3)_{1-x}$ arise.

The formation of the $CuInSe_2$ compound by the above process thus appears to obey the following reaction mechanism which is similar to that reported for the formation of $CuInSe_2$ by the annealing of stacked elemental layers where all the individual layers were deposited by thermal evaporation [18]. Cu and In are provided from the solid phases of $Cu_{11}In_9$, CuIn, $Cu_{16}In_9$ and Cu_9In_4 and also from the liquid phases of Cu and In (if present) and they react with Se to produce binary selenides. For annealing

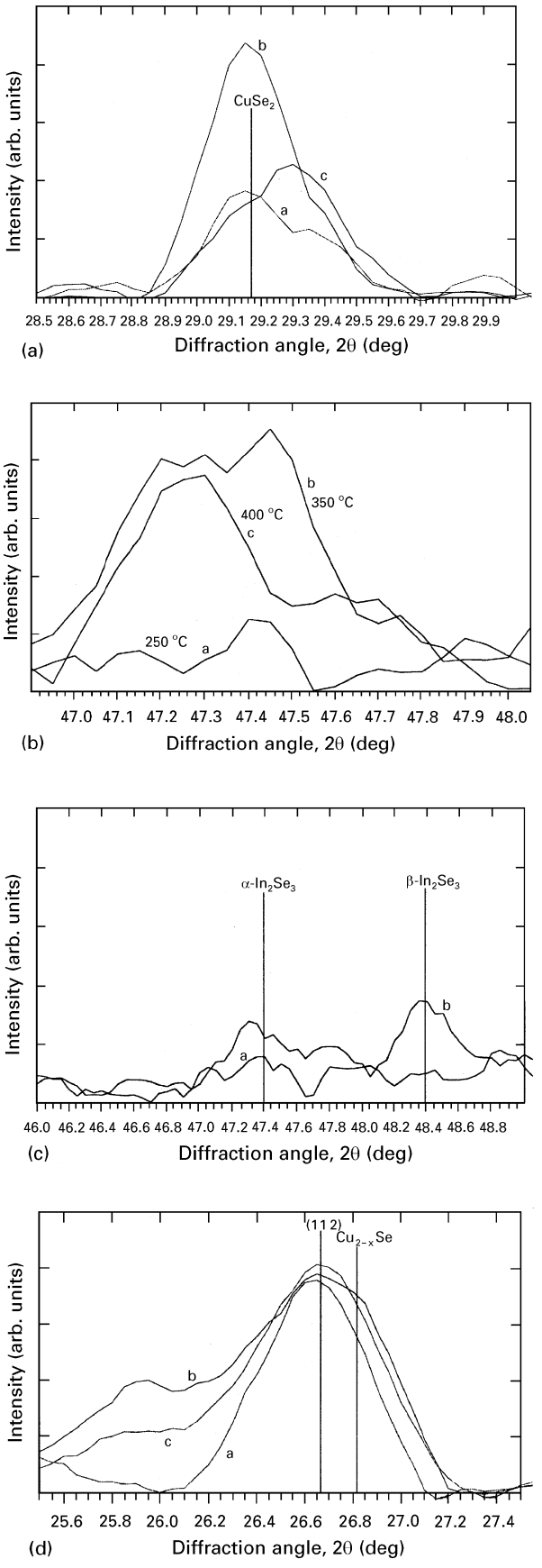

Figure 6 (a) Variation of the intensity of the $CuSe_2$ peak with annealing temperatures of (a) 150 °C, (b) 200 °C and (c) 250 °C and (b) variation of the intensity of the α-In_2Se_3 peak with annealing temperatures of (a) 250 °C, (b) 350 °C and (c) 400 °C and (c) variation of α-In_2Se_3 and β-In_2Se_3 peak intensities with annealing temperatures of (a) 200 °C and (b) 300 °C and (d) Variation of the intensity of the Cu_2Se peak with annealing temperatures of (a) 250 °C, (b) 350 °C and (c) 450 °C. (The figures are not drawn to the same scale).

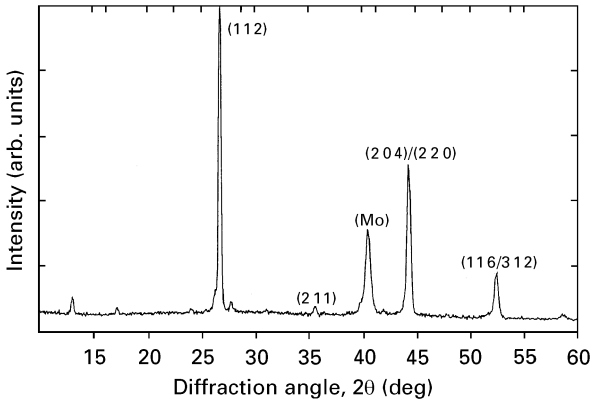

Figure 7 XRD pattern of the $CuInSe_2$ film annealed at 550 °C.

temperatures $t < 200$ °C, Cu preferentially reacts with Se rather than In to produce $CuSe_2$:

$$Cu + 2Se \rightarrow CuSe_2 \quad (1)$$

Above 200 °C, In reacts with Se to form α-In_2Se_3 which at higher temperatures partially transforms to β-In_2Se_3.

$$2In + 3Se \rightarrow \alpha\text{-}In_2Se_3 \quad (2)$$

$$\alpha\text{-}In_2Se_3 \rightarrow \beta\text{-}In_2Se_3 \quad (3)$$

The above result that Cu, rather than In, reacts preferentially with Se at lower temperatures closely agrees with the observations of Sachan and Meakin [19].

For annealing temperatures between 250–400 °C, the Se-rich copper selenides transform into Cu-rich selenides with the possible following exothermic reactions that involve a considerable loss of Se.

$$2CuSe_2 \rightarrow 2CuSe + Se_2\ (g) \quad (4)$$

$$4CuSe \rightarrow 2Cu_2Se + Se_2\ (g) \quad (5)$$

and finally, at 400 °C and above, Cu_2Se reacts with In_2Se_3 to form $CuInSe_2$ via the reaction:

$$Cu_2Se + In_2Se_3 \rightarrow 2CuInSe_2 \quad (6)$$

It should be noted that Yamanaka *et al.* [20] and Verma *et al.* [21] have reported that InSe, In_2Se and Cu_7Se_4 and elemental In in the Cu–In precursors are selenized in the above temperature range and thus they suggested a different reaction mechanism scheme for the formation of $CuInSe_2$.

Another feature that can be observed from the XRD spectra is the shift in position and distortion in shape of the characteristic (1 1 0) peak of Mo. Fig. 8 shows the variation in the position of the (1 1 0) Mo peak with annealing temperature. It can be seen that there is a considerable change in the Mo peak position and also the full width at half maximum (FWHM) values of the peaks vary with annealing temperature which indicates the presence of strains in the Mo layer that changes with annealing. The d value for the (1 1 0) Mo peak has been calculated for the samples using standard relations and the strain values in the films were calculated using the following formula [16]:

$$\varepsilon = \frac{d_{\text{strained}} - d_{\text{unstrained}}}{d_{\text{unstrained}}} \quad (7)$$

where $d_{\text{unstrained}}$ has been taken to be the value obtained for the precursor. The strain values, ε, thus obtained for different films are shown in Fig. 9(a), while the peak positions in the diffraction angle scale are shown in Fig. 9(b). There are two possible reasons for the generation of strains in the Mo layer; (i) a large difference in the thermal expansion coefficient values between the Cu–In alloy and the $CuInSe_2$ compound

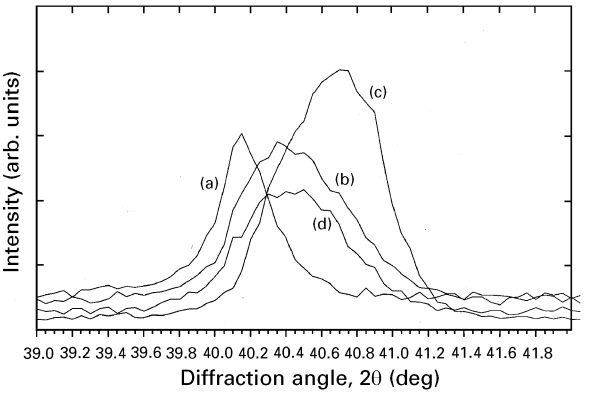

Figure 8 Position of the Mo (1 1 0) peak in films annealed at temperatures of (a) 200 °C, (b) 300 °C, (c) 450 °C and (d) 500 °C.

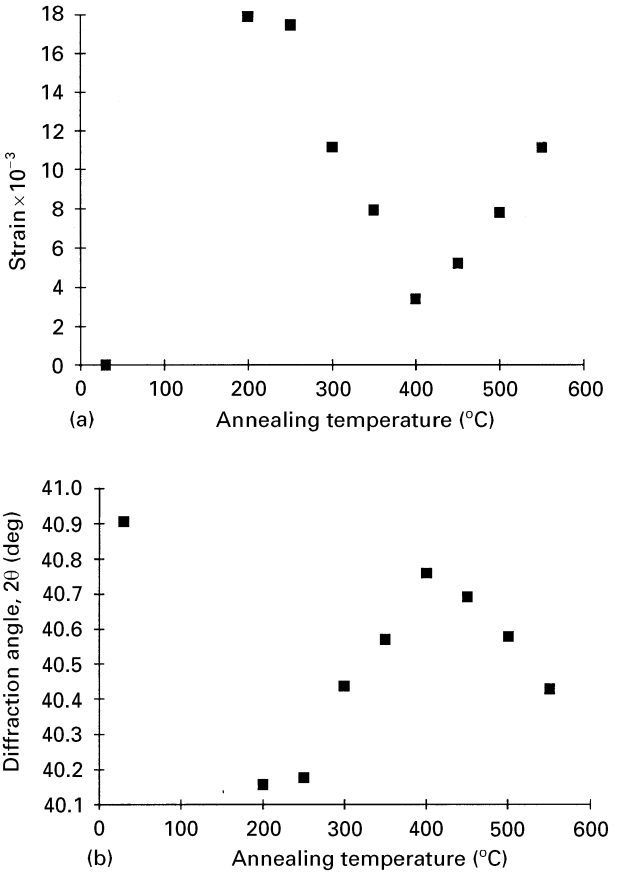

Figure 9 Variation of the (a) the strain in the Mo layers with annealing temperatures (Values at 30 °C correspond to the precursor) and (b) the Mo (1 1 0) peak positions.

and (ii) a volume expansion of $CuInSe_2$ in the process of selenization [22]. It is found that for samples with an evaporated Se layer that are annealed at 150 °C, a significant volume expansion takes place due to the incorporation of Se in the Cu–In precursor and the Mo peak shifts to a relatively lower value. The peak shifts move gradually to higher values for films annealed in the temperature range of 200–400 °C reflecting a decrease in the strain in the films with increasing annealing temperature. However, there is still significant tensile strain present in the films annealed at 400 °C, which again increases with any further increase in the annealing temperature. This is possibly due to the mismatch between thermal expansion coefficient values of the Cu–In alloy layer and the $CuInSe_2$ compound. The Mo layers are heated along with the Cu–In layer on its surface but it cools down after the $CuInSe_2$ layer has formed. The value of the tensile strain at 450 °C, as found from Fig. 9, closely matches the value calculated theoretically (3.4×10^{-3}). The thermal expansion coefficient, α, values for the Cu–In alloys and $CuInSe_2$ used in the calculations are taken from reference [16] (α for $CuInSe_2$ is $9.0 \times 10^{-6}\,°C^{-1}$ and for the Cu–In alloy layer it is $17.0 \times 10^{-6}\,°C^{-1}$). This also closely agrees with the previously discussed model for the formation of $CuInSe_2$ on selenization.

4. Conclusion

Chalcopyrite structured $CuInSe_2$ films with a strong (1 1 2) orientation have been obtained on Mo coated glass substrates by annealing a stack consisting of single layers of sputtered Cu and In and an overlying evaporated Se layer. $Cu_{11}In_9$ has been found to be the major phase present in the precursor, however other Cu–In phases e.g., CuIn, $Cu_{16}In_9$ and Cu_9In_4 are also evolved at different ranges of annealing temperature before they react with Se. Binary phases of Cu_2Se, $CuSe_2$ and In_2Se_3 are found to appear in samples annealed at intermediate temperature ranges which finally react to form the ternary phase of $CuInSe_2$. The reaction of Cu has been found to occur with Se at a relatively lower temperature than that for In with Se. It has been found that there is a significant amount of Se incorporation into the Cu–In precursor annealed in the temperature range (~100–200 °C). However, as the annealing temperature is increased, there is a considerable amount of Se loss for samples annealed up to about 400 °C where the films are found to reach the stoichiometry and definite crystalline orientation of chalcopyrite $CuInSe_2$. The Se incorporation is accompanied by a volume expansion of the deposited layer which results in considerable tensile strain on the underlying Mo layer causing a shift in the characteristic (1 1 0) peak of Mo towards 2θ values. The amount of this shift decreases with an increase in the annealing temperature due to possible Se loss from the sample. However, a certain amount of shift in the Mo peak is still found to be present for samples annealed at 400 °C and above due to the difference in the thermal expansion coefficient values of the Cu–In binary phases and the ternary $CuInSe_2$.

References

1. J. KESSLER, S. WEIDEMAN, L. RUSSELL, T. LOMMASSON, S. SKIBO, J. FOGLEBOCH, T. CLOSS and R. R. ARYA, in Proceedings of the 24th IEEE Photovoltaic Special Conference (1994) 206.
2. A. M. GABOR, J. R. TUTTLE, M. CONTRERAS, D. S. ALBIN, A. FRANZ, D. W. NILES and R. NOUFI, in Proceedings of the 12th European Photovoltaic Solar Energy Conference (1994) 939.
3. B. M. BASOL, V. K. KAPUR and A. HALANI, in Proceedings of the 22nd IEEE Photovoltaic Special Conference (1991) 893.
4. K. MITCHELL, C. EBERSPACHER, J. ERMER and D. PIER, in Proceedings of the 20th IEEE Photovoltaic Special Conference (1988) 1384.
5. W. E. DAVANEY, R. A. MICKELSEN and W. S. CHEN, in Proceedings of the 18th IEEE Photovoltaic Special Conference (1985) 1733.
6. R. A. MICKELSEN and W. S. CHEN, in Proceedings of the 15th IEEE Photovoltaic Special Conference (1981) 800.
7. T. W. WALTER, M. J. CARTER and R. HILL, in Proceedings of the 9th European Photovoltaic Solar Energy Conference (1989) 115.
8. A. VARVAET, M. BURGELMAN, I. CLEMMINCK and J. CAPON, *ibid.* p. 480.
9. A. KNOWLES, H. OUMOUS, M. J. CARTER and R. HILL, in Proceedings of the 20th IEEE Photovoltaic Special Conference (1988) 1482.
10. N. ROMEO, V. CANEVERI, G. SBERVEGLIERI, A. BOSIO and L. ZANOTTI, *Solar Cells* **16** (1986) 155.
11. J. A. THRONTON, D. G. CORNOG, R. B. HALL, S. P. SHEA and J. D. MEAKIN, *J. Vac. Sci. Technol.* **A2** (1984) 307.
12. R. R. ARYA, T. LOMMASSON, B. FIESELMANN, L. RUSSELL, L. CARR and A. CATALANO, in Proceedings of the 22nd IEEE Photovoltaic Special Conference (1991) 903.
13. T. NAKADA, K. MIGITA and A. KUNIOKA, in Proceedings of the 23rd IEEE Photovoltaic Special Conference (1993) 560.
14. R. W. BIRKMIRE, L. C. DINETTA, P. G. LASSWELL, J. D. MEAKIN and J. E. PHILIPS, *Solar Cells* **16** (1986) 419.
15. H. DITTRICH, U. PRINZ, J. SZOT and H. W. SCHOCK, in Proceedings of the 9th European Photovoltaic Solar Energy Conference (1989) 163.
16. D. ALBIN, J. CARAPELLA, A. DUDA, J. TUTTLE, A. TENNANT, R'NOUFI and B. M. BASOL, in Proceedings of the 22nd IEEE Photovoltaic Special Conference (1991) 907.
17. S. P. KUMAR, R. B. GORE, S. K. KULKARNI and R. K. PANDEY, *Thin Solid Films* **208** (1992) 161.
18. F. O. ADURODIJA, Ph.D. thesis, University of Northumbria at Newcastle, Newcastle Upon Tyne, UK (1994).
19. V. SACHAN and J. D. MEAKIN, *Sol. En. Mater and Solar Cell* **30** (1993) 147.
20. S. YAMANAKA, B. E. MACCANDLESS and R. W. BIRKMIRE, in Proceedings of the 23rd IEEE Photovoltaic Special Conference (1993) 607.
21. S. VERMA, S. YAMANAKA, R. W. BIRKMIRE, B. E. MACCANDLESS and T. W. F. RUSSEL, in Proceedings of the 11th IEEE European Photovoltaic Solar Energy Conference (1992) 807.
22. K. ZWEIBEL, H. S. ULLAL and R. L. MITCHELL, in Proceedings of the 21st IEEE Photovoltaic Special Conference (1990) 458.

Received 18 August 1995
and accepted 21 October 1996